Time-resolved phase-space tomography of an optomechanical cavity

Oren Suchoi, Keren Shlomi, Lior Ella, and Eyal Buks
Department of Electrical Engineering, Technion, Haifa 32000 Israel
(Received 12 August 2014; published 20 April 2015)

We experimentally study the phase-space distribution (PSD) of a mechanical resonator that is simultaneously coupled to two electromagnetic cavities. The first one, operating in the microwave band, is employed for inducing either cooling or self-excited oscillation (SEO), whereas the second one, operating in the optical band, is used for displacement detection. A tomography technique is employed for extracting the PSD from the signal reflected by the optical cavity. Measurements of PSD are performed in steady state near the threshold of SEO while sweeping the microwave cavity detuning. In addition, we monitor the time evolution of the transitions from an optomechanically cooled state to a state of self-excited oscillation. This transition is induced by abruptly switching the microwave driving frequency from the red-detuned region to the blue-detuned one. The experimental results are compared with theoretical predictions that are obtained by solving the Fokker-Planck equation. The feasibility of generating quantum superposition states in the system under study is briefly discussed.

DOI: 10.1103/PhysRevA.91.043829 PACS number(s): 42.50.Wk, 03.65.Wj, 07.10.Cm, 85.85.+j

Optomechanical cavities are currently a subject of intense basic and applied study [1–7]. These devices can be employed in various sensing [8–13] and photonics applications [14–22]. Moreover, optomechanical cavities may allow experimental study of the crossover from classical to quantum mechanics [2,23–33] and the observation of macroscopic quantum behavior in mechanical systems [25,27,29,32,34–49]. When the finesse of the optical cavity that is employed for constructing the optomechanical cavity is sufficiently high, the coupling to the mechanical resonator that serves as a vibrating mirror is typically dominated by the effect of radiation pressure [2,6,23,50–55]. On the other hand, bolometric effects can contribute to the optomechanical coupling when optical absorption by the vibrating mirror [56–59] is significant [7,57–66]. In recent years a variety of cavity optomechanical systems have been constructed and studied [2,4–6,7,23,32,33,41,50,52,55,67–72] and phenomena such as mode cooling [32,67,71–73], self-excited oscillation (SEO) [4,24,56,58,62,70,74–76], and optically induced transparency [77–80] have been investigated.

In this work we study experimentally a hybrid system made of a single mechanical resonator and two cavities, one operating in the microwave band and the other in the optical band. We study SEO induced by driving the microwave cavity in the blue-detuned region. The technique of state tomography is employed in order to construct the phase-space distribution (PSD) of the mechanical resonator [81], whose displacement is detected using the optical cavity. We begin by mapping out the PSD in steady state near the threshold of SEO. We then employ time-resolved measurements of PSD for both studying the drifting in time of the phase of SEO and monitoring the transition from cooling to SEO. In the latter case, the frequency of the driving signal that is injected into the microwave cavity is abruptly switched from the red-detuned region to the blue-detuned one, allowing thus the recording of the time evolution from an initial state, in which the mechanical resonator is cooled down, to a final state, in which the system undergoes SEO. The possibility of employing such abrupt switching for the creation of quantum superposition states is briefly discussed.

The experimental setup is schematically depicted in Fig. 1. A photolithography process is used to pattern a microwave microstrip cavity made of 200-nm-thick aluminum on a high-resistivity silicon wafer. At the open end of the microstrip, a mechanical resonator in the shape of a $100 \times 100\ \mu\text{m}^2$ trampoline supported by four beams is fabricated [66]. At the other end, the microwave cavity is weakly coupled to a feedline, which guides both the injected and reflected microwave signals. Details of the fabrication process can be found elsewhere [82].

The sample is mounted inside a closed Cu package, which is internally coated with Nb. Measurements are performed in a dilution refrigerator operating at a temperature of 0.54 K and in vacuum. The injected microwave signal is first attenuated by a 20-dB directional coupler at the same temperature before entering the feedline. The reflected microwave signal is amplified using a cryogenic amplifier at 4 K and measured in both the frequency domain (using a network analyzer and a spectrum analyzer) and in the time domain (using a power diode connected to an oscilloscope). The fundamental microwave cavity resonance frequency is $f_c = \omega_c/2\pi = 2.783$ GHz, the corresponding linear damping rate is $\gamma_c = 4.2$ MHz, the fundamental mechanical resonance frequency is $f_m = \omega_m/2\pi = 662.7$ kHz, and the corresponding mechanical linear damping rate is $\gamma_m = 2.5$ Hz.

A single-mode optical fiber coated with Nb is placed above the suspended trampoline (see Fig. 1). In the presence of the coated fiber, two optomechanical cavities are formed: One is a superconducting cavity operating in the microwave band and the other is a fiber-based cavity operating in the optical band. The coupling between the mechanical resonator and the microwave cavity, originating by the capacitance between the coated fiber and the suspended trampoline [82], is dominated by the effect of radiation pressure, whereas bolometric effects are responsible for the coupling between the mechanical resonator and the optical cavity. The fact that both optomechanical cavities share the same mechanical resonator can be exploited for inducing mechanically mediated coupling between microwave and optical photons [83–91].

A fiber Bragg grating (FBG) mirror and a focusing lens are made near the fiber tip. To allow optical transmission,

 ©2015 American Physical Society

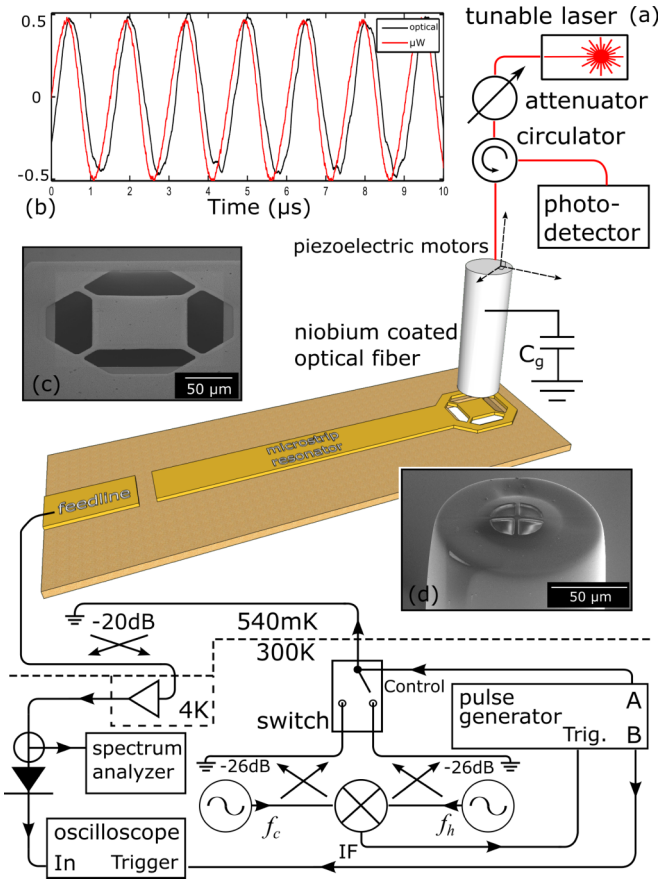

FIG. 1. (Color online) Experimental setup. (a) Dual optomechanical cavity. The microwave cavity is a superconducting microstrip made of aluminum over a high-resistivity silicon wafer coated with a 100-nm-thick SiN layer. The optomechanical coupling is generated using a Nb-coated optical fiber that is positioned at a submicron distance from the trampoline. The optical setup (seen above the sample) allows using the optical cavity for displacement detection, whereas the microwave setup (seen below the sample) is employed for exciting the microwave cavity and measuring its response. For the measurements of PSD in steady state, a single microwave synthesizer is employed, whereas for the time-resolved measurements, two synthesizers (tuned to frequencies f_c, and f_h, respectively) are used together with a pulse generator in order to ensure a smooth switching from cooling to heating. (b) Off-reflected signals of both the optical and the microwave cavities, in the region where the system exhibits SEO in steady state. (c) The mechanical resonator at the end of the microstrip is shown in the electron micrograph. Several windows are opened in the Nb layer on the fiber tip using FIB, as can be seen in (d).

the core of the fiber at the tip is exposed by etching the Nb coating using a focused ion beam (FIB) [82]. A cryogenic piezoelectric three-axis positioning system having subnanometer resolution is employed for manipulating the position of the optical fiber. The reflected signal off the optical cavity, which is measured both by a spectrum analyzer and by an oscilloscope, is employed for displacement detection. A tunable laser operating near the Bragg wavelength $\lambda_B = 1545.8$ nm of the FBG together with an external attenuator is employed to excite the optical cavity. Optical absorption by the suspended mirror may give rise to heating, which in turn may causes thermal deformation of the suspended structure due to mismatch between thermal expansion coefficients of the suspended mirror made of aluminum and the supported silicon substrate [64]. With relatively intense input laser power such bolometric coupling may result in a variety of optomechanical backreaction effects [66]. In order to avoid such effects [65], the input laser power feeding the optical cavity is kept at sufficiently low level (below 60 μW), allowing the utilization of the optical cavity for displacement detection without any significant effect on the dynamics of other parts of the system.

Self-excited oscillation can be induced by injecting a monochromatic pump signal into the feedline of the microwave cavity provided the angular frequency of the pump signal ω_p is blue detuned with respect to the angular cavity resonance frequency ω_c, i.e., provided $\omega_p > \omega_c$, and provided the injected power P_p exceeds a threshold value. Figure 1(b) shows time traces of the off-reflected signals of both the optical and the microwave cavities in the region where the system exhibits SEO induced by a microwave monochromatic pump tone having normalized detuning $d = (\omega_p - \omega_c)/\omega_m = 0.7$ and power $P_p = 0.63$ μW. The off-reflected optical signal is measured using a photodetector and the off-reflected microwave signal is measured using a power diode. The relative phase between the two oscillating signals allows the direct measurement of the retardation [92] in the response of the microwave cavity to mechanical oscillation (note that the retardation in the response of the optical cavity is negligibly small).

The PSD provides important insight into the effect of noise on the dynamics of the system under study in both the classical and quantum regimes. In a recent theoretical work Nation studied an optomechanical cavity (with radiation-pressure-based coupling) and demonstrated that under appropriate conditions the steady-state Wigner quasiprobability PSD in the region of SEO may exhibit some signatures for nonclassicality [93]. Armour and Rodrigues [94] have found that in the semiclassical approximation (in which third-order derivative terms in the equation of motion for the Wigner function are neglected) the master equation leads to Langevin equations corresponding to the classical dynamics of the system. Furthermore, the assumption that the dynamics of the mechanical resonator is slow on the time scale of the cavity dynamics allows employing the technique of adiabatic elimination in order to derive an evolution equation for the complex amplitude A of the mechanical resonator, which is found to be given by

$$\dot{A} + (i\Omega_{\rm eff} + \Gamma_{\rm eff})A = \xi(t), \tag{1}$$

where both the effective angular resonance frequency detuning $\Omega_{\rm eff}$ and the effective damping rate $\Gamma_{\rm eff}$ are real even functions of $A_r \equiv |A|$. To second order in A_r they are expressed as $\Omega_{\rm eff} = \omega_0 + \omega_2 A_r^2$ and $\Gamma_{\rm eff} = \gamma_0 + \gamma_2 A_r^2$. The fluctuating term [95] $\xi(t) = \xi_x(t) + i\xi_y(t)$, where both ξ_x and ξ_y are real, represents white noise and the following is assumed to hold: $\langle \xi_x(t)\xi_x(t')\rangle = \langle \xi_y(t)\xi_y(t')\rangle = 2\Theta\delta(t-t')$ and $\langle \xi_x(t)\xi_y(t')\rangle = 0$, where $\Theta = \gamma_m k_B T_{\rm eff}/4m\omega_m^2$, k_B is the Boltzmann constant. and $T_{\rm eff}$ is the effective noise temperature.

In the absence of optomechanical coupling $\Omega_{\rm eff}$ and $\Gamma_{\rm eff}$ represent the angular resonance frequency detuning (with respect to ω_m) and the damping rate of the isolated mechanical

resonator, i.e., $\Omega_{\rm eff} = \omega_0 = 0$ and $\Gamma_{\rm eff} = \gamma_0 = \gamma_{\rm m}$, respectively. However, with a finite optomechanical coupling both $\Omega_{\rm eff}$ and $\Gamma_{\rm eff}$ are modified when the cavity is externally driven. Consider the case where a monochromatic tone having normalized amplitude $a_{\rm p}$ and angular frequency $\omega_{\rm p}$ is injected into the feedline in order to drive the microwave cavity. For this case the effective linear angular frequency detuning ω_0 and the effective linear damping rate γ_0 become $\omega_0 = 2G^2E_{\rm c}\omega_{\rm m}^{-1}\,{\rm Im}\,\Xi_1$ and $\gamma_0 = \gamma_{\rm m} + 2G^2E_{\rm c}\omega_{\rm m}^{-1}\,{\rm Re}\,\Xi_1(d,g)$, respectively, where $\Xi_l(d,g) = [-i(d+l)+g]^{-1} + [-i(d-l)-g]^{-1}$, $g = \gamma_{\rm c}/\omega_{\rm m}$ is the normalized cavity damping rate, and $E_{\rm c}$ is the average number of photons in the cavity in steady state, which is related to $a_{\rm p}$ by $E_{\rm c} = |a_{\rm p}|^2\omega_{\rm m}^{-2}(d^2+g^2)^{-1}$ when optomechanical coupling is disregarded [94,96]. The optomechanical coupling constant G represents the shift in the effective cavity angular resonance frequency induced by displacing the mechanical resonator by its zero-point amplitude.

In the current study we focus on the region close to the threshold of SEO, for which the effect of resonance frequency detuning $\Omega_{\rm eff}$ can be disregarded. For such a case the Langevin equation (1) for the complex amplitude A can be expressed in a two-dimensional vector form as $\dot{\mathbf{A}} + \nabla\mathcal{H} = \boldsymbol{\xi}$, where $\mathbf{A} = (A_x, A_y)$, A_x and A_y are the real and imaginary parts of A, respectively, the noise term is $\boldsymbol{\xi} = (\xi_x, \xi_y)$, and the scalar function $\mathcal{H}$ is given by $\mathcal{H} = (\gamma_0/2)A_r^2 + (\gamma_2/4)A_r^4$ [97,98]. The corresponding Fokker-Planck equation for the PSD $\mathcal{P}$ can be written as [95]

$$\frac{\partial\mathcal{P}}{\partial t} - \nabla\cdot(\mathcal{P}\nabla\mathcal{H}) - \Theta\nabla\cdot(\nabla\mathcal{P}) = 0. \qquad (2)$$

Consider the case where $\gamma_2 > 0$, for which a supercritical Hopf bifurcation occurs when the linear damping coefficient γ_0 vanishes. Above threshold, i.e., when γ_0 becomes negative, the amplitude A_r of SEO is given by $A_{r0} = \sqrt{-\gamma_0/\gamma_2}$. The Fokker-Planck equation (2) can be used to evaluate the normalized PSD function in steady state $W(A)$, which is found to be given by $W = Z^{-1}e^{-\mathcal{H}/\Theta}$, where Z is a normalization constant (partition function) [95,98,99]. Note that W is independent of the angle A_θ of the complex variable A.

Figure 2(a) exhibits the measured PSD in steady state as a function of the normalized detuning d with a fixed pump power of $P_{\rm p} = 0.63\ \mu$W. The PSD is extracted from the measured displacement of the mechanical resonator, i.e., from the off-reflected signal of the optical cavity, using the technique of state tomography [99,100]. Both the measured PSD [Fig. 2(a)] and the calculated one [Fig. 2(b)] are plotted vs the normalized radial amplitude $A_r/\delta_{\rm m}$, where $\delta_{\rm m} = \sqrt{2\Theta/\gamma_{\rm m}}$. The device parameters that have been employed for generating the theoretical plot are listed in the figure caption. As d is increased from its initial value in the blue-detuning regime, the mechanical element loses its stability due to the interaction with the microwave cavity and undergoes a supercritical Hopf bifurcation at $d = 0.474$. When d is further increased, the energy stored in the cavity is diminished and the optomechanical coupling becomes smaller, until eventually the system regains its stability at $d = 1.06$. No hysteresis is found at this power level when d is swept upward and downward. Note that the measured PSD [see Fig. 2(a)] exhibits larger width around the average value [in comparison to theory; see Fig. 2(b)] due to added measurement noise of displacement detection.

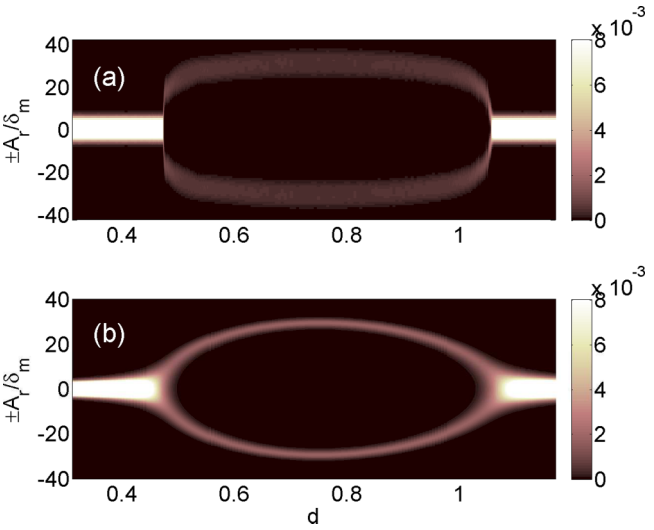

FIG. 2. (Color online) The PSD in steady state as a function of the normalized detuning d. (a) Measured PSD extracted using the technique of state tomography. (b) Calculated PSD obtained from the steady-state solution of Eq. (2). The lower parts of both panels with negative A_r are mirror reflections of the upper parts with positive A_r. The following device parameters have been employed in the calculation: $G = 0.013$ Hz (corresponding to frequency shift per displacement of 55 MHz $\mu{\rm m}^{-1}$) and $\gamma_2\delta_{\rm m}^2\gamma_{\rm m}^{-1} = 2.0\times10^{-4}$. The rate of nonlinear damping γ_2 is taken to be independent of the cavity driving parameters since the optomechanical contribution to γ_2 is found to be negligibly small.

The phase of SEO in steady state randomly drifts in time due to the effect of external noise. In addition, noise gives rise to amplitude fluctuations around the average value A_{r0}. To experimentally study these effects SEO is driven by injecting a monochromatic pump tone having normalized detuning $d = 0.7$ and power $P_{\rm p} = 0.77\ \mu$W into the feedline. The off-reflected signal from the optical cavity is recorded in two time windows separated by a dwell time $t_{\rm d}$. While the data taken in the first time window are used to determined the initial amplitude and phase of SEO, the data taken in the second one are used to extract the PSD using tomography. The results are shown in Fig. 3 for four different values of the dwell time $t_{\rm d}$. While the left panels show the measured PSDs, the panels on the right exhibit the calculated PSDs obtained by numerically integrating the Fokker-Planck equation (2). For the longest dwell time the phase of SEO becomes nearly random and consequently the PSD becomes nearly independent of the angle A_θ.

While cavity excitation in the measurements of the PSD in steady state is performed using a single microwave synthesizer, the time-resolved experiment, in which the transition from cooling to heating is recorded, is performed using two synthesizers. The first one, having negative normalized detuning $d_1 = -0.475$, serves during the cooling stage, whereas the second one, having the opposite normalized detuning $d_2 = -d_1$, is employed for driving SEO. Both synthesizers are connected to an rf switch through two -26-dB directional couplers. The attenuated signal from the couplers is connected to the

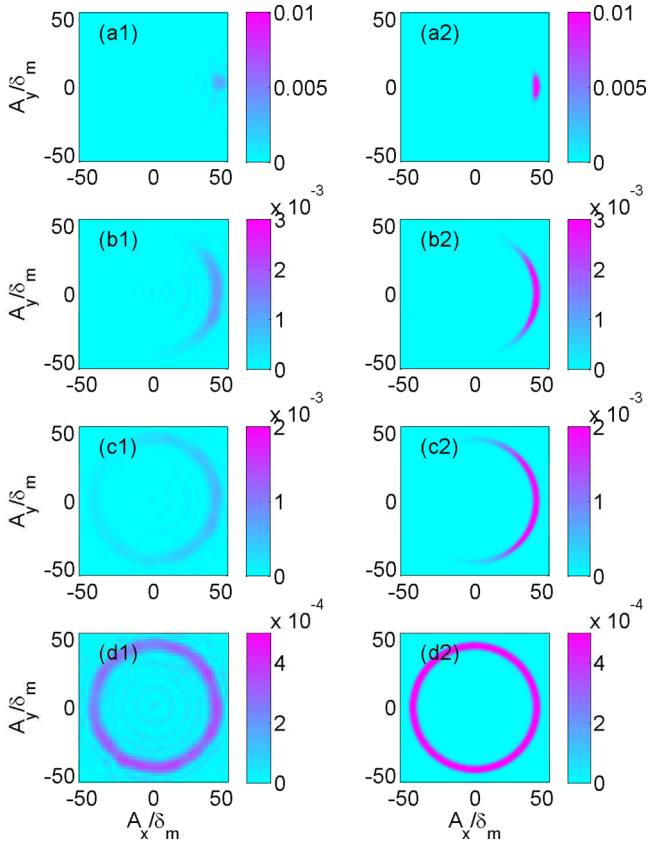

FIG. 3. (Color online) (a1)–(d1) Measured and (a2)–(d2) calculated PSD in steady-state SEO. The normalized dwell time $\gamma_m t_d$ is (a) 0.12, (b) 1.2, (c) 7.5, and (d) 12.

input ports of a microwave switch, while the through signal from the two synthesizers is mixed using an rf mixer. The intermediate-frequency port of the mixer is used for triggering a pulse generator, which in turn triggers the rf switch. Both the time delay between the two triggers and the power levels of both synthesizers are carefully tuned in order to achieve a smooth transition from cooling to heating. This is done by monitoring the off-reflected signal shortly after switching and by minimizing signal ringing. A smooth transition is achieved when both the amplitude and phase of the cavity fixed point before switching coincide with the amplitude and phase corresponding to the cavity fixed point after switching (which is unstable). Note that the relative phase is a periodic function of the time delay with a period given by the inverse frequency difference between the two synthesizers $\pi/d_2\omega_m = 1\ \mu$s. The power level of both synthesizers is set close to 1.0 μW (with fine adjustments to eliminate ringing).

Figure 4 shows the PSD as a function of the normalized delay time $\gamma_m t$, where t is the elapsed time since the switching from cooling to heating. For each measurement, the cavity is first excited with normalized detuning d_1 for 5 s, a time duration that is sufficiently long to reach steady state in the cooling stage. The off-reflected signal from the optical cavity is employed for extracting the PSD using tomography. Figure 4(a) shows the measured PSD, whereas Fig. 4(b) shows the calculated PSD, which is obtained by numerically integrating the Fokker-Planck equation (2). Note that the PSD

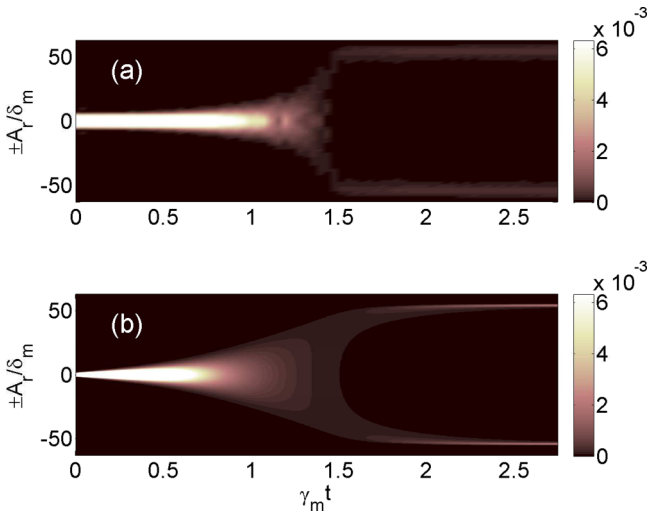

FIG. 4. (Color online) Time-resolved PSD as a function of the normalized elapsing time $\gamma_m t$ since the switching from cooling to heating: (a) measured PSD and (b) calculated PSD, which is obtained by numerically integrating the Fokker-Planck equation (2). The lower parts of both panels with negative A_r are mirror reflections of the upper parts with positive A_r.

is expected to be independent of the angle A_θ of the complex variable A provided the transition from cooling to heating is smooth.

An analytical approximation to the time evolution of $\mathcal{P}$ that is generated by the Fokker-Planck equation (2) can be obtained for the case of short delay times $t > 0$, for which A_r is sufficiently small to allow disregarding the effect of nonlinear damping. For this case, $\mathcal{P}$ is found to be a Gaussian distribution given by $\mathcal{P} = \pi^{-1}\delta_H^{-2}\exp(-A_r^2/\delta_H^2)$, with exponentially growing width δ_H given by

$$\delta_H = \sqrt{\frac{2\Theta}{\gamma_{ba}+\gamma_m}\left(1+\frac{2\gamma_{ba}(e^{2(\gamma_{ba}-\gamma_m)t}-1)}{\gamma_{ba}-\gamma_m}\right)}, \qquad (3)$$

where $\gamma_{ba} = 2G^2E_c\omega_m^{-1}\,\mathrm{Re}\,\Xi_1(d_1,g)$ is the backaction contribution to the mechanical damping rate.

The process of the PSD expansion, which is triggered by switching cavity detuning from cooling to heating, can be employed under appropriate conditions for the generation of a quantum superposition state [39,94] (see the Appendix). Increasing the value of γ_{ba} by increasing the power injected into the microwave cavity allows both enhancement of cooling efficiency before switching and acceleration of the PSD expansion after switching [see Eq. (3)]. The latter is highly desirable since experimental observation of a superposition state is possible only if the time needed to generate the state is shorter than the corresponding decoherence time. On the other hand, while nonlinearity in the response of the microwave cavity has been disregarded in the data analysis presented above, such effects may play an important role at higher power levels [82,101–105]. Taking full advantage of nonlinearity for enhancing the efficiency of cooling [103] and for the suppression of decoherence [96] may open the way for experimental exploration of nonclassicality at a macroscopic scale in such systems.

This work was supported by the Israel Science Foundation, the Bi-National Science Foundation, the Security Research Foundation at Technion, the Israel Ministry of Science, the Russell Berrie Nanotechnology Institute, and MAFAT.

APPENDIX: FEASIBILITY OF EXPERIMENTAL OBSERVATION OF NONCLASSICALITY

The switching of cavity detuning from cooling to heating triggers a process of isotropic expansion of the PSD [see Eq. (3)]. Experimental observation of nonclassicality during this process is expected to become possible only when some conditions are satisfied. Below, the feasibility of satisfying these conditions is discussed. The analysis is based on some simplifying assumptions. The effective cavity Kerr coefficient [96] is assumed to be sufficiently small to allow disregarding nonlinearity in the cavity response. The optomechanical cavity is assumed to operate in the resolved sideband regime, i.e., it is assumed that $g = \gamma_c/\omega_m \ll 1$. For that case cooling is optimized with normalized cavity detuning of $d = (\omega_p - \omega_c)/\omega_m = -1$ and heating is optimized with $d = 1$. Furthermore, it is assumed that $n_m \equiv k_B T/\hbar\omega_m \gg 1$, $n_c \equiv k_B T/\hbar\omega_c \ll 1$, $\gamma_c/\omega_c \ll 1$, and $\gamma_m/\omega_m \ll 1$.

The characteristic width $\delta_H(t)$ of the state that is generated at time t after the switching is given by Eq. (3). Equation (99) of Ref. [96] is employed in order to estimate the decoherence time τ_φ of the state. The assumptions that $1 \ll \mathcal{E}_c \ll \min(\omega_m/g\gamma_m, 1/g^2)$ and that ground-state cooling is reached prior to the switching lead to

$$\frac{1}{\tau_\varphi} \simeq 4\gamma_m[1 + 2(e^{4\mathcal{E}_c\gamma_m t} - 1)]n_m, \tag{A1}$$

where

$$\mathcal{E}_c = \frac{E_c G^2}{\gamma_c\gamma_m} \simeq \frac{\gamma_{ba}}{2\gamma_m}. \tag{A2}$$

Detection of quantum coherence is possible only when the time needed to generate the state t is shorter than the corresponding decoherence time τ_φ. Hence, the generation of a macroscopic quantum superposition state, i.e., a state having width δ_H that is significantly larger than the width corresponding to the ground state, is possible only when

$$\mathcal{E}_c \gtrsim n_m. \tag{A3}$$

As an example, for the parameters of the device that has been used in Ref. [106] to demonstrate the coherent state transfer between itinerant microwave fields and a mechanical oscillator, for which $\gamma_c\gamma_m n_m/G^2 \simeq 1.5 \times 10^4$ and $\hbar\omega_c\gamma_c \simeq 10^{-14}$ mW, condition (A3) imposes a lower bound on the input power given by $P_p \gtrsim 10^{-10}$ mW. For such a power level the assumption that cavity nonlinearity can be disregarded is likely to be valid with a common superconducting microwave cavity. Thus, we conclude that with state-of-the-art devices macroscopic quantum superposition states can be generated using our proposed protocol.

[1] V. Braginsky and A. Manukin, Zh. Eksp. Teor. Fiz. **52**, 986 (1967) [Sov. Phys. JETP **25**, 653 (1967)].
[2] S. Gigan, H. R. Böhm, M. Paternostro, F. Blaser, J. B. Hertzberg, K. C. Schwab, D. Bauerle, M. Aspelmeyer, and A. Zeilinger, Nature (London) **444**, 67 (2006).
[3] F. Marquardt and S. M. Girvin, Physics **2**, 40 (2009).
[4] K. Hane and K. Suzuki, Sensors Actuators A **51**, 179 (1996).
[5] C. M. I. Favero, S. Camerer, D. Konig, H. Lorenz, J. P. Kotthaus, and K. Karrai, Appl. Phys. Lett. **90**, 104101 (2007).
[6] T. J. Kippenberg and K. J. Vahala, Science **321**, 1172 (2008).
[7] C. H. Metzger and K. Karrai, Nature (London) **432**, 1002 (2004).
[8] O. Arcizet, P.-F. Cohadon, T. Briant, M. Pinard, A. Heidmann, J.-M. Mackowski, C. Michel, L. Pinard, O. Français, and L. Rousseau, Phys. Rev. Lett. **97**, 133601 (2006).
[9] V. Braginsky and F. Khalili, *Quantum Measurement* (Cambridge University Press, Cambridge, 1995).
[10] A. Clerk, M. Devoret, S. Girvin, F. Marquardt, and R. Schoelkopf, Rev. Mod. Phys. **82**, 1155 (2010).
[11] S. Forstner, S. Prams, J. Knittel, E. D. van Ooijen, J. D. Swaim, G. I. Harris, A. Szorkovszky, W. P. Bowen, and H. Rubinsztein-Dunlop, Phys. Rev. Lett. **108**, 120801 (2012).
[12] D. Rugar, H. J. Mamin, and P. Guethner, Appl. Phys. Lett. **55**, 2588 (1989).
[13] S. Stapfner, L. Ost, D. Hunger, J. Reichel, I. Favero, and E. M. Weig, Appl. Phys. Lett. **102**, 151910 (2013).
[14] M. Bagheri, M. Poot, M. Li, W. P. H. Pernice, and H. X. Tang, Nat. Nanotechnol. **6**, 726 (2011).
[15] G. Bahl, J. Zehnpfennig, M. Tomes, and T. Carmon, Nat. Commun. **2**, 403 (2011).
[16] M. Eichenfield, C. P. Michael, R. Perahia, and O. Painter, Nat. Photon. **1**, 416 (2007).
[17] N. Flowers-Jacobs, S. Hoch, J. Sankey, A. Kashkanova, A. Jayich, C. Deutsch, J. Reichel, and J. Harris, Appl. Phys. Lett. **101**, 221109 (2012).
[18] M. Hossein-Zadeh and K. J. Vahala, IEEE J. Sel. Top. Quantum Electron. **16**, 276 (2010).
[19] S. E. Lyshevski and M. Lyshevski, *Proceedings of the Third IEEE Conference on Nanotechnology, 2003* (IEEE, Piscataway, 2003), Vol. 2, pp. 840–843.
[20] N. Stokes, F. Fatah, and S. Venkatesh, Electron. Lett. **24**, 777 (1988).
[21] M. C. Wu, O. Solgaard, and J. E. Ford, J. Lightwave Technol. **24**, 4433 (2006).
[22] X. Zhou, F. Hocke, A. Schliesser, A. Marx, H. Huebl, R. Gross, and T. J. Kippenberg, Nat. Phys. **9**, 179 (2013).
[23] O. Arcizet, P.-F. Cohadon, T. Briant, M. Pinard, and A. Heidmann, Nature (London) **444**, 71 (2006).
[24] T. Carmon, H. Rokhsari, L. Yang, T. J. Kippenberg, and K. J. Vahala, Phys. Rev. Lett. **94**, 223902 (2005).
[25] C. Genes, D. Vitali, P. Tombesi, S. Gigan, and M. Aspelmeyer, Phys. Rev. A **77**, 033804 (2008).
[26] A. M. Jayich, J. C. Sankey, B. M. Zwickl, C. Yang, J. D. Thompson, S. M. Girvin, A. A. Clerk, F. Marquardt, and J. G. E. Harris, New J. Phys. **10**, 095008 (2008).
[27] H. J. Kimble, Y. Levin, A. B. Matsko, K. S. Thorne, and S. P. Vyatchanin, Phys. Rev. D **65**, 022002 (2001).

[28] P. Meystre, Ann. Phys. (Berlin) **525**, 215 (2013).
[29] M. Poot and H. S. van der Zant, Phys. Rep. **511**, 273 (2012).
[30] A. Schliesser, R. Riviere, G. Anetsberger, O. Arcizet, and T. J. Kippenberg, Nat. Phys. **4**, 415 (2008).
[31] H. Tang and D. Vitali, Phys. Rev. A **89**, 063821 (2014).
[32] J. D. Teufel, D. Li, M. S. Allman, K. Cicak, A. J. Sirois, J. D. Whittaker, and R. W. Simmonds, Nature (London) **471**, 204 (2011).
[33] J. Thompson, B. Zwickl, A. Jayich, F. Marquardt, S. Girvin, and J. Harris, Nature (London) **452**, 72 (2008).
[34] M. Bahrami, M. Paternostro, A. Bassi, and H. Ulbricht, Phys. Rev. Lett. **112**, 210404 (2014).
[35] A. Farace, F. Ciccarello, R. Fazio, and V. Giovannetti, Phys. Rev. A **89**, 022335 (2014).
[36] C. Galland, N. Sangouard, N. Piro, N. Gisin, and T. J. Kippenberg, Phys. Rev. Lett. **112**, 143602 (2014).
[37] Q. Y. He and M. D. Reid, Phys. Rev. A **88**, 052121 (2013).
[38] S. Kiesewetter, Q. Y. He, P. D. Drummond, and M. D. Reid, Phys. Rev. A **90**, 043805 (2014).
[39] N. Lörch, J. Qian, A. Clerk, F. Marquardt, and K. Hammerer, Phys. Rev. X **4**, 011015 (2014).
[40] C. P. Meaney, R. H. McKenzie, and G. J. Milburn, Phys. Rev. E **83**, 056202 (2011).
[41] A. D. O'Connell, M. Hofheinz, M. Ansmann, R. C. Bialczak, M. Lenander, E. L. M. Neeley, D. Sank, H. Wang, M. Weides, J. Wenner *et al.*, Nature (London) **464**, 697 (2010).
[42] T. Palomaki, J. Teufel, R. Simmonds, and K. Lehnert, Science **342**, 710 (2013).
[43] I. Pikovski, M. R. Vanner, M. Aspelmeyer, M. Kim, and Č. Brukner, Nat. Phys. **8**, 393 (2012).
[44] J. Qian, A. A. Clerk, K. Hammerer, and F. Marquardt, Phys. Rev. Lett. **109**, 253601 (2012).
[45] D. A. Rodrigues and A. D. Armour, Phys. Rev. Lett. **104**, 053601 (2010).
[46] S. Walter, A. Nunnenkamp, and C. Bruder, Phys. Rev. Lett. **112**, 094102 (2014).
[47] A. J. Weinstein, C. U. Lei, E. E. Wollman, J. Suh, A. Metelmann, A. A. Clerk, and K. C. Schwab, Phys. Rev. X **4**, 041003 (2014).
[48] X. Xu, M. Gullans, and J. M. Taylor, Phys. Rev. A **91**, 013818 (2015).
[49] X.-W. Xu, H. Wang, J. Zhang, and Y.-x. Liu, Phys. Rev. A **88**, 063819 (2013).
[50] T. Corbitt, Y. Chen, E. Innerhofer, H. Müller-Ebhardt, D. Ottaway, H. Rehbein, D. Sigg, S. Whitcomb, C. Wipf, and N. Mavalvala, Phys. Rev. Lett. **98**, 150802 (2007).
[51] T. J. Kippenberg, H. Rokhsari, T. Carmon, A. Scherer, and K. J. Vahala, Phys. Rev. Lett. **95**, 033901 (2005).
[52] D. Kleckner and D. Bouwmeester, Nature (London) **444**, 75 (2006).
[53] E. F. Nichols and G. F. Hull, Phys. Rev. (Series I) **13**, 307 (1901).
[54] H. Rokhsari, T. Kippenberg, T. Carmon, and K. Vahala, Opt. Express **13**, 5293 (2005).
[55] A. Schliesser, P. Del'Haye, N. Nooshi, K. J. Vahala, and T. J. Kippenberg, Phys. Rev. Lett. **97**, 243905 (2006).
[56] K. Aubin, M. Zalalutdinov, T. Alan, R. Reichenbach, R. Rand, A. Zehnder, J. Parpia, and H. Craighead, J. Microelectromech. Syst. **13**, 1018 (2004).
[57] S. De Liberato, N. Lambert, and F. Nori, Phys. Rev. A **83**, 033809 (2011).
[58] F. Marquardt, J. G. E. Harris, and S. M. Girvin, Phys. Rev. Lett. **96**, 103901 (2006).
[59] M. Paternostro, S. Gigan, M. S. Kim, F. Blaser, H. R. Böhm, and M. Aspelmeyer, New J. Phys. **8**, 107 (2006).
[60] G. Jourdan, F. Comin, and J. Chevrier, Phys. Rev. Lett. **101**, 133904 (2008).
[61] F. Marino and F. Marin, Phys. Rev. E **83**, 015202(R) (2011).
[62] C. Metzger, M. Ludwig, C. Neuenhahn, A. Ortlieb, I. Favero, K. Karrai, and F. Marquardt, Phys. Rev. Lett. **101**, 133903 (2008).
[63] J. Restrepo, J. Gabelli, C. Ciuti, and I. Favero, C. R. Phys. **12**, 860 (2011).
[64] D. Yuvaraj, M. B. Kadam, O. Shtempluck, and E. Buks, J. Micromech. Syst. **22**, 430 (2013).
[65] S. Zaitsev, O. Gottlieb, and E. Buks, Nonlinear Dyn. **69**, 1589 (2012).
[66] S. Zaitsev, A. K. Pandey, O. Shtempluck, and E. Buks, Phys. Rev. E **84**, 046605 (2011).
[67] J. Chan, T. Alegre, A. Safavi-Naeini, J. Hill, A. Krause, S. Gröblacher, M. Aspelmeyer, and O. Painter, Nature (London) **478**, 89 (2011).
[68] T. Corbitt and N. Mavalvala, J. Opt. B **6**, S675 (2004).
[69] S. Gröblacher, J. T. Hill, A. H. Safavi-Naeini, J. Chan, and O. Painter, Appl. Phys. Lett. **103**, 181104 (2013).
[70] C. Regal, J. Teufel, and K. Lehnert, Nat. Phys. **4**, 555 (2008).
[71] J. Teufel, T. Donner, D. Li, J. Harlow, M. Allman, K. Cicak, A. Sirois, J. Whittaker, K. Lehnert, and R. Simmonds, Nature (London) **475**, 359 (2011).
[72] S. Gröblacher, J. B. Hertzberg, M. R. Vanner, G. D. Cole, S. Gigan, K. Schwab, and M. Aspelmeyer, Nat. Phys. **5**, 485 (2009).
[73] A. Schliesser, O. Arcizet, R. Rivière, G. Anetsberger, and T. Kippenberg, Nat. Phys. **5**, 509 (2009).
[74] T. Carmon and K. J. Vahala, Phys. Rev. Lett. **98**, 123901 (2007).
[75] T. Corbitt, D. Ottaway, E. Innerhofer, J. Pelc, and N. Mavalvala, Phys. Rev. A **74**, 021802 (2006).
[76] K. Kim and S. Lee, J. Appl. Phys. **91**, 4715 (2002).
[77] M. Karuza, C. Biancofiore, M. Bawaj, C. Molinelli, M. Galassi, R. Natali, P. Tombesi, G. Di Giuseppe, and D. Vitali, Phys. Rev. A **88**, 013804 (2013).
[78] T. Ojanen and K. Borkje, Phys. Rev. A **90**, 013824 (2014).
[79] A. H. Safavi-Naeini, T. P. M. Alegre, J. Chan, M. Eichenfield, M. Winger, Q. Lin, J. T. Hill, D. E. Chang, and O. Painter, Nature (London) **472**, 69 (2011).
[80] S. Weis, R. Riviere, S. Deleglise, E. Gavartin, O. Arcizet, A. Schliesser, and T. J. Kippenberg, Science **330**, 1520 (2010).
[81] M. R. Vanner, I. Pikovski, and M. Kim, Ann. Phys. (Berlin) **527**, 15 (2015).
[82] O. Suchoi, L. Ella, O. Shtempluk, and E. Buks, Phys. Rev. A **90**, 033818 (2014).
[83] R. W. Andrews, R. W. Peterson, T. P. Purdy, K. Cicak, R. W. Simmonds, C. A. Regal, and K. W. Lehnert, Nat. Phys. **10**, 321 (2014).
[84] J. Bochmann, A. Vainsencher, D. D. Awschalom, and A. N. Cleland, Nat. Phys. **103**, 122602 (2013).
[85] B. D. Clader, Phys. Rev. A **90**, 012324 (2014).
[86] K. Y. Fong, L. Fan, L. Jiang, X. Han, and H. X. Tang, Phys. Rev. A **90**, 051801(R) (2014).

[87] C. Jiang, Y. Cui, H. Liu, and G. Chen, arXiv:1404.3928.
[88] L. Tian, Ann. Phys. (Berlin) **527**, 1 (2015).
[89] Y.-D. Wang, S. Chesi, and A. A. Clerk, Phys. Rev. A **91**, 013807 (2015).
[90] X.-B. Yan, W. Z. Jia, Y. Li, and J.-H. Wu, arXiv:1405.6506.
[91] Z.-q. Yin, W. L. Yang, L. Sun, and L. M. Duan, Phys. Rev. A **91**, 012333 (2015).
[92] V. B. Braginsky, M. L. Gorodetsky, F. Y. Khalili, and K. S. Thorne, Phys. Rev. D **61**, 044002 (2000).
[93] P. D. Nation, Phys. Rev. A **88**, 053828 (2013).
[94] A. D. Armour and D. A. Rodrigues, C. R. Phys. **13**, 440 (2012).
[95] H. Risken, *The Fokker-Planck Equation: Methods of Solution and Applications* (Springer, Berlin, 1996).
[96] E. Buks, C. R. Phys. **13**, 454 (2012).
[97] I. Baskin, D. Yuvaraj, G. Bachar, K. Shlomi, O. Shtempluck, and E. Buks, J. Micromech. Syst. **23**, 563 (2014).
[98] R. D. Hempstead and M. Lax, Phys. Rev. **161**, 350 (1967).
[99] Y. Dhayalan, I. Baskin, K. Shlomi, and E. Buks, Phys. Rev. Lett. **112**, 210403 (2014).
[100] K. Vogeland H. Risken, Phys. Rev. A **40**, 2847 (1989).
[101] K. Børkje, A. Nunnenkamp, J. D. Teufel, and S. M. Girvin, Phys. Rev. Lett. **111**, 053603 (2013).
[102] T. Dahmand D. J. Scalapino, J. Appl. Phys. **81**, 2002 (1997).
[103] P. D. Nation, M. P. Blencowe, and E. Buks, Phys. Rev. B **78**, 104516 (2008).
[104] O. Suchoi, B. Abdo, E. Segev, O. Shtempluck, M. P. Blencowe, and E. Buks, Phys. Rev. B **81**, 174525 (2010).
[105] B. Yurkeand E. Buks, J. Lightwave Technol. **24**, 5054 (2006).
[106] T. Palomaki, J. Harlow, J. Teufel, R. Simmonds, and K. Lehnert, Nature (London) **495**, 210 (2013).